Re-entrant Transformation Methods in Closed Cell Foams

Martz, E. O., Lee, T., Lakes, R. S., Goel, V. K. and Park, J. B. "Re-entrant transformation methods in closed cell foams", adapted from *Cellular Polymers*, 15, 229-249, (1996).

Rod Lakes, University of Wisconsin

Abstract

Open-cell foams have been transformed in prior studies, to a re-entrant (inward bulging) cell structure which gives rise to a negative Poisson's ratio. Different methods were used for polymer foams with and without a softening point. In this study, methods based on air pressure were developed for the transformation of closed cell polymer foams. Low density polyethylene foam was successfully transformed,howeverpolymethacrylimide foam was densified without transformation.

Introduction

Poisson's ratio relates the strain in the lateral direction to that of the strain in the longitudinal direction. For a homogeneous, isotropic structure,

$$\nu_{xy} = -\frac{\varepsilon_y}{\varepsilon_x} \tag{1}$$

Here, ε_x is the strain applied in the x direction, and ε_y is the resultant tensile strain in the y direction, which is transverse with respect to the x direction. For isotropic materials, $\nu_{xy} = \nu_{yx} \equiv \nu$.

Based on theoretical energy arguments presented by Fung(1), the range of Poisson's ratio that isotropic materials may possess is between $-1.0 \leq \nu \leq 0.5$. For anisotropic materials, values outside this range are possible. An isotropic material having a negative Poisson's ratio, however, was not believed to exist until recent work by Lakes(2). The fabrication of such foam materials was achieved through a transformation of the cell structure from a convex polyhedral shape to a concave shape. These transformed foam samples exhibiting a negative Poisson's ratio have been termed "re-entrant" due to the inward bulging of the cell ribs. Prior experiments in preparing and studying re-entrant polyurethane foam (Scott industrial foam)(2-4) and silicone rubber foam(3) dealt exclusively with open cell foams. Different transformation techniques were used for each of these materials.

Based on the theory of linear elasticity, four constants are used to describe an isotropic material's behavior in the elastic realm: shear modulus (G), Young's modulus (E), bulk modulus (K), and Poisson's ratio (ν). Only two of these four are independent; from these two, the remaining one may be determined The equation relating the shear modulus to Young's modulus and Poisson's ratio is presented below.

$$G = \frac{E}{2(1+\nu)} \tag{2}$$

One can see that as the Poisson's ratio approaches -1.0, the shear modulus will greatly exceed Young's modulus. The material becomes extremely difficult to shear, but is also comparatively more compliant or resilient in compression or tension. Indeed, Lakes(2) observed that his negative Poisson's ratio foams were more resilient (with a smaller value for Young's modulus) than their conventional counterparts. The latter followed a nearly linear relation between compressive stress and strain for up to 5%, whereas the re-entrant foams exhibited this type of relationship for up to 40% strain.

For most materials, the shear modulus is two times (ν ú 0) to three times (ν ú 0.5) greater than Young's modulus; most commonly though, ν ú 0.3. Poisson's ratio also is used to relate the shear modulus to the bulk modulus, which describes the ease of volumetric deformation.

$$G = \frac{3K(1-2\nu)}{2(1+\nu)} \tag{3}$$

Rubber, which has a Poisson's ratio of close to 0.5, is termed incompressible because the bulk modulus greatly exceeds the shear modulus. However, as $\nu \to -1.0$, the material becomes much easier to compress. In some engineering applications such material properties that arise from materials exhibiting a negative Poisson's ratio are desirable: enhanced shear moduli, indentation resistance, and fracture toughness(2).

The rationale for making closed cell foams re-entrant is as follows. One can envision an application for a closed cell foam, such as polyethylene, as part of an artificial intervertebral disc, which upon compression would not bulge outward to impinge on any nearby nerves. Another possible application is a foam core for sandwich panels of the type used in aircraft; closed cell polymethacrylimide (Rohacell®) is used in such an application. Re-entrant core materials could be used for damping vibrations and sound, as well as achieving resistance to impact damage.

This paper describes the transformation of closed cell polymethacrylimide (PMI) and low density polyethylene (LDPE) foams in an attempt to impose re-entrant structures on them. New methods of achieving permanent, triaxial compression were developed. A cylindrical pressure chamber was designed to compress the foam in three orthogonal directions simultaneously. The specimens were transformed using high external pressures and near softening temperatures, and the material properties of the deformed specimens were subsequently analyzed.

Experimental Procedures

(1) Materials

Two types of closed cell foam materials were used: polymethacrylimide (PMI) Rohacell® and low density polyethylene (LDPE) Ethafoam®.

Polymethacrylimide (PMI)

Polymethacrylimide foams, with a closed cell structure, were obtained from a commercial manufacturer (Rohacell®, Rohm Tech Inc. Malden, MA). This structurally isotropic PMI foam is composed of a rigid polymer which can resist high temperatures and pressures, 180˚C and 690 kPa, respectively. Various samples of the PMI foams were used, with the density of the foams given in Table 1. The 51 WF grade foam was mainly used for this study. The original foams were provided in blocks (110 cm x 220 cm x 5 cm; width, length, and height respectively), but they were cut into cubes (2 cm x 2 cm x 2 cm) with a band saw for easier processing. Then, parallel-to-axis planes were marked to facilitate measurements of the actual dimensions of the materials. Additional specimens measuring 2.5 cm x 2.5 cm x 8 cm in width, length and height respectively, were made from the 51 WF foam. These geometrically similar, high-aspect ratio specimens were used in mechanical tests which could be performed later in accordance with Saint-Venant's principle(5).

Low Density Polyethylene (LDPE)

Three types of closed cell LDPE foams were obtained from a commercial manufacturer (Ethafoam®, Foamcraft Inc., Chicago, IL) with densities given in Table 1. Initial trials indicated that the Ethafoam® samples were anisotropic after processing, therefore the foam samples were cut to approximately 2.5 x 2.5 x 5.0 cm, with the long side being the direction of maximum compression during transformation. Again,parallel-to-axis planes were marked to measure the actual dimensions of the materials. Permanent deformation was quantified using a micrometer to measure dimensions before and after transformation. Volumetric compression factors were inferred from these measurements.

(2) Methods of Transformation

It was desired to permanently compress the foam in three orthogonal directions simultaneously. A technique was developed to expose heated samples to high external air pressures. It was assumed that since the foam was closed-cell, high external pressure would provide a very uniform, triaxial compression. A special pressure chamber was designed based on the analytical stress distribution of a thick-walled cylinder and was manufactured in the Engineering Machine Shop.

The heating source used in this portion of the study was a passive convection furnace (Isotemp® Model No. 126, Fisher Scientific Co., Pittsburgh, PA). A copper-constantan thermocouple wire (Omega, Model No. HH23, Stamford, CT) was placed inside the chamber to measure temperature. During the oven ramp-up period, temperature inside the chamber initially showed a significant difference with respect to the furnace temperature indicator. This delay is attributed to the lag due to heat capacity and thermalconductivity between oven air and chamber air through the 19 mm thick chamber wall.

To estimate the required pressure, calculations based on the ideal gas law were performed to obtain initial values for the air pressure. The rationale is that the hydrostatic pressure applied must overcome the pressure of the gas within the closed cells in addition to the stiffness of the foam skeleton. The calculated cell gas pressure therefore represents a lower bound on the required external pressure at a given temperature. Assuming that a volumetric compression factor of 3 would be sufficient to achieve $\nu < 0$ in polymer(2, 4) foams, and based on previous work, a trial softening temperature of 170˚C was used, the lower bound of pressure was calculated to be 455 kPa. It should be noted, however, that the ideal gas law does not contain a "time" variable. Many preliminary trials were attempted to find an optimal time constant for achieving permanent volumetric compression in order to obtain the re-entrant property of the foams.

In compressing the LDPE, the same pressure chamber and furnace as described above were utilized. Making similar use of the ideal gas law to determine a lower bound for the pressure, and knowing that the softening temperature of the LDPE foam is about 75˚C, the lower bound of pressure was determined to be 360 kPa. The specimens were subjected to heat and pressure for 10 hours, after which time the heat was turned off, while a constant pressure continued to be applied for an additional 6 hours.

It was reasoned that by using vacuum pressure and heat, a re-entrant structure in these LDPE foams might be achieved by an alternate method. If the closed cell foam specimens were to be heated to their softening point, and a vacuum pressure applied, then the gas trapped within the cells can expand as a result of both the heat and the favorable pressure gradient. This line of reasoning assumes that the gas entrapped within each cell is able to diffuse through the cell walls. Upon an increase of pressure to atmospheric, buckling of the cell ribs is expected to occur, producing the re-entrant structure.

LDPE foam samples of similar size and shape to those described above were prepared for transformation by the vacuum method. Measuring the size and deformation of these samples was done in the same manner as previously described. The oven was heated to the desired temperature, at which time the specimens were placed in the oven and allowed to soften for approximately 1 hour. The air within the oven chamber was then evacuated and this pressure was held for 5 minutes. After air had been reintroduced back into the oven, thereby restoring atmospheric pressure, the specimens were removed from the oven and allowed to cool. The volumetric compression factor was quantified using a micrometer.

(3) Evaluation of Mechanical Properties and Poisson's Ratio

Evaluation of the mechanical properties of PMI foams were conducted using a micromechanics apparatus capable of performing torsion and bending tests upon small specimens. The micromechanics apparatus was used to determine the Young's modulus and shear modulus of the PMI foams, and from these, one can calculate the Poisson's ratio. This device, as illustrated in Figure 2, has been discussed in greater detail in previous literature(6-8). Testing coupons were made by cutting 2 mm x 3 mm x 12 mm sections from reduced specimens, meeting the required size for the equipment. Five samples each of untransformed and transformed foams were measured for Young's modulus and shear modulus. The PMI foam samples were transformed under either 170˚C or 220˚C heating conditions with 552 kPa applied pressure and 8 hours heating time.

The Poisson's ratio for the transformed LDPE foam specimens was determined by measuring lateral and longitudinal strains due to an applied longitudinal stress. After the transformation the samples were cored (a knife was used to remove the outer layer from all sides), and from this core, two specimens were obtained for tension tests. Cores from specimens prepared using both methods of transformation were studied. Two specimens were attached to a thin strip of copper via Duco® Cement (Devcon Corp., Wood Dale, IL) on one end, and on the other end of the samples, separate pieces of copper were attached. On the latter ends, a piece of ribbon was inserted between the copper and the LDPE foam sample for attachment of dead weights. A series of weights was hung from the ribbon to generate uniaxial tension loads. The resultant axial and lateral displacements were measured based on reference marks on the samples using a digital micrometer. An untransformed piece of LDPE HS 45, cut in a similar manner to the transformed pieces, was used as a control and subjected to the same type of tension tests. Due to the much lower stiffness of the LDPE foam, in comparison to the PMI foam, direct determination of Young's modulus and Poisson's ratio of the LDPE foam was considered more appropriate.

(4) Optical and Scanning Electron Microscopic (SEM) Observations

Two types of PMI foam samples were used for the Scanning Electron Micrograph (SEM) evaluation. One original and two transformed foams of type 51 WF were included in the study, as well as an original type 300 WF for comparison. The type 51 WF samples included specimens deformed at temperatures of 170°C and 220°C. A Hitachi "Nature" SEM (Model No. S-2460N at Central Electron Microscopy Research Facility) was used for the study. An accelerating voltage of 3 kV was used to take micrographs of the samples which were sputter coated with Au-Pd.

A light microscope was used to observe any changes in the cell wall geometry as a result of the processing to induce a re-entrant structure in the LDPE foam samples. Slices approximately 3 mm thick were cut from the transformed foam samples of LDPE HS 45. Samples from both methods of transformation were viewed under low magnification.

Results

(1) Heating and Compression

Uniform, three-dimensional volumetric compression of PMI 51 WF foam was achieved by air pressure and furnace heating of specimens inside the pressure chamber. Differences in volumetric compression factors (defined as the ratio of final relative density to intial relative density, with relative density defined as the ratio of the density of the foam to the density of the material composing the foam) were not noteworthy between heating times of 8 to 20 hours, therefore, the shortest heating period (8 hours) was used. The highest volumetric compression factor occurred at an air pressure of 552 kPa. The specimens compressed at 170˚C had a near-uniform volumetric compression factor of 2.0 over the entire heating time span, but this did appear to rise slightly with longer heating times. Reduction in volume was much greater in the specimens compressed at the higher temperature of 220˚C. The volumetric compression factor increased with heating duration, and leveled off at 8.0 after 12 hours of heating time. An attempt was made to reduce the foam at 250˚C, however due to severe charring of the first few specimens, transformation measurements at this temperature were not deemed possible and further trials at this temperature were abandoned.

The HS 45 Ethafoam® foams achieved a re-entrant structure after undergoing compression and heat at 621 kPa and 105˚C, as well as 621 kPa and 110˚C, both for 10 hours, followed by 6 hours of pressure alone. In coring the sample, a transition region (or density gradient) between the outer, non-re-entrant foam, and the inner, re-entrant foam was observed. This density gradient observed in one of the transformed foams (110˚C and 621 kPa) was quantified. The original relative density of the foam was 0.07 and the overall volumetric compression factor of the entire foam immediately after it was transformed was 1.44. In the inner, central region, the volumetric compression factor was 2.41, and in the outer region this value was 1.36.

Three weeks later the volumetric compression factor of this foam was again measured and it was found that further compression occurred. The inner, central region exhibited a volumetric compression factor of 3.38 and the value for the outer region was 1.89. A simple, one dimensional diffusion model, with a diffusion coefficient of air (taken to be 20% O_2 and 80% N_2) through LDPE calculated to be $3.48\text{x}10^{-7}$ cm^2/sec(9), was used to examine this phenomena of continued shrinkage. The thickness of a cell wall within the LDPE foam was measured under a microscope and determined to be 4.3 μm. Additionally, a cubic volume was assumed for the model, which was equivalent in volume to the 2.5 cm x 2.5 cm x 5.0 cm sample that was transformed. The model predicted that diffusion through a cubic, LDPE foam sample would occur over approximately 19 days. This was in good agreement with what was observed, and it was reasoned that residual stresses remaining in the cell structure after the transformation process drove the diffusion of gas within the cells out through the foam sample. These transformed samples behaved as closed-cell foams. Attempts to blow air through the transformed LDPE HS 45 foam disclosed no obvious transmission of air.

Similar to the foams treated using hydrostatic pressure, the vacuum treated foams manifested their re-entrant effect only after being cored. The relative density of the inner and outer portions of one of the vacuum transformed samples (86˚C and -86 kPa) was measured. The original relative density of this foam was 0.07, and after the transformation the overall volumetric compression factor of the sample was 2.21. The inner, central region yielded a volumetric compression factor of 2.73, and the outer region had a value of 1.73. After three weeks, there was no continued shrinkage observed in this sample. In contrast to the method by which the re-entrant cell structure was achieved in the hydrostatically applied pressure trials, a combination of vacuum pressure, heat, and then atmospheric pressure has been shown to be capable of producing a re-entrant structure. It is suggested that the re-entrant structure results from the expansion of both the air trapped within the cell walls, as well as the softening of the cell ribs and walls, so that they too stretch, as the gas that they entrap expands. The pressure gradient established by the vacuum will also contribute to the expansion of the gas within the cells. After the cell walls and ribs have been stretched, the reintroduction of atmospheric pressure will cause these walls and ribs to buckle, thus producing the re-entrant structure.

Summaries of the processing sequences and their respective volumetric compression factors obtained as a result of the specific processing, are provided in Tables 2 & 3.

(2) Evaluation of Mechanical Properties and Poisson's Ratio

Two samples of PMI 51 WF foam were transformed at the same pressure and for the same duration (552 kPa in 8 hours time) while varying the processing temperature (170˚C and 220˚C). As stated previously, those foams deformed under 170˚C temperatures showed concave surfaces. At higher temperatures (220˚C), however, the specimens appeared uniformly reduced in three directions without any irregularities. It can be concluded that a specimen transformed at a lower temperature has a reduction rate slower than at higher temperature. The specimens resulting in curved surfaces may be ones in mid-transformation.

The resulting color of the reduced PMI specimens was also intriguing. From an original foam color of snow white, the transformed foams possessed a darker, yellowish color. The color was more extreme at higher heating temperatures, however, this coloring was limited in depth from the surface, and the core still appears white. Oxidation may have occurred on the surface during the compression stage without any effect on the inner specimen material.

Table 4 shows for each specimen of PMI foam the average Young's modulus, E, the shear modulus, G, the calculated Poisson's ratio if the materials were isotropic, and their corresponding densities. Young's modulus and shear modulus values were calculated using equations for beams under bending and torsion(5). There was a large standard deviation in the resulting Young's modulus values. This may be caused in part by higher specimen end motion during bending in comparison with torsion. Hence the Young’s modulus is more susceptible to noise than the shear modulus is.

The resulting material property data were plotted in Figure 3 with respect to processing temperatures. Both Young's modulus and shear modulus increased with higher processing temperatures. For a re-entrant structure, Young's modulus should decrease and shear modulus should increase slightly, according to earlier work done by Lakes(2). Based on his observations, the present closed-cell PMI 51 WF foam does not have his definition of a re-entrant structure, and thus has a positive Poisson's ratio. These values show the Poisson's ratio (calculated from the isotropic relation in eqtn. 2) to exhibit a small decrease from 0.39 to 0.33, but this is still positive.

The density of transformed 51 WF foam was 0.191 g/cm^3, which is similar to untransformed 200 WF type PMI foam, 0.205 g/cm^3. The Young's modulus of transformed 51 WF foam exhibits a slightly smaller value than untransformed 200 WF (Table 4); the shear modulus is considerably smaller. Therefore, the transformation procedures creates a denser and stiffer foam from the original lower density 51 WF foam; but there seems to be no advantage in comparison with the 200 WF grade which is denser as received.

The major conclusions drawn from this study of the PMI foams were that three-dimensional compression of closed-cell structure did not give rise to a re-entrant structure with the techniques used. Unlike the open-cell structure, the closed cell walls tended to become thicker and sometimes break instead of folding when transformed, as can be seen in the SEM pictures. The transformed structure, however, exhibited a higher density which can be compared with the untransformed higher density grade foams (i.e. 200 WF).

Superficially, it seemed that the transformed LDPE HS 45 foam specimens did not achieve an amount of volumetric compression necessary to induce a re-entrant structure, however, what appeared on the outside was deceiving. A sample from the core of the foam was extracted by slicing the outer layer of the foam away from the core. It was found that this cored sample exhibited a negative Poisson's ratio in one direction upon being pulled. This phenomenon was observed in both the foams treated by hydrostatic as well as by vacuum pressure, however, in the stiffer foams (HS 600 and HS 900), such an effect was not noticed.

Results from the tension tests to determine the Poisson's ratio of the re-entrant and untransformed LDPE foams are presented in Figures 4 - 6. Each graph shows the value of Poisson's ratio as a function of axial strain, based on measurements taken using a digital micrometer. Fractional error bars were based on the resolution of the human eye (0.1 mm), which was considered to be the limiting factor in determining the Poisson's ratio. These results demonstrate a negative Poisson's ratio, clearly showing that as one applies an axial tensile strain, lateral expansion occurs. It appears that the best method to achieve re-entrant effects is through a combination of heat plus hydrostatic pressure. Where no error bars are shown, they are smaller than the size of the data points.

(3) Optical and Scanning Electron Microscopic Observations

Figure 7 shows a micrograph of an untransformed type 51 WF PMI closed-cell structure. Cell walls can be easily discerned and depth of surfaces are viewed with darker gray. Thickening of the cell walls can be clearly distinguished in the transformed (170˚C, 552 kPa, 8 hours heating) sample, shown in Figure 8. From this micrograph, one can see relatively thick struts of the transformed foam which correspond to higher densities. Some cell walls showed crevices and voids caused by the transformation procedure. No significant bulge-in property (i.e. re-entrant structure of the cell walls), was observed, in agreement with the micromechanics results.

Figure 9 shows micrographs of a highly transformed type 51 WF PMI foam (220˚C, 552 kPa, 8 hours heating) and Figure 10 shows a high density, virgin 300 WF foam. From these photos, one can easily note similarities in the shapes. Some cells ruptured in transformation, resulting in dark apertures as seen in the transformed foam micrographs. In comparison to the previous micrograph, this sample shows a more compressed structure, although no significant re-entrant characteristic can be viewed. The SEM photos reveal that transformed PMI foams only increased in density, but did not exhibit the microstructure indicative of materials with a negative Poisson's ratio.

Upon microscopic evaluation of LDPE foam slices, there appeared to be cell rib buckling in the samples of HS 45, for both methods of transformation. Figures 11 - 13 show representative pictures of original LDPE HS 45 foams, and HS 45 foams from both the transformation processes. The negative Poisson's ratio effect was noticed when a sample from the core of the transformed foams was examined. There was a gradient effect of cell rib buckling, in the sense that the outer portions appeared to exhibit some degree of buckling, while the cell ribs of the inner regions were thoroughly buckled. The unfolding of the re-entrant cells when one pulls on the foam was observed under a microscope to be very graphic. The unfolding of the kinked cells is the causal mechanism that is responsible for the resultant negative Poisson's ratio(2). However, these foams exhibited a negative Poisson's ratio in only one direction, which confirmed the belief that they were anisotropic in nature. In the foams that were successfully made re-entrant using vacuum pressure, as well as hydrostatic pressure, there existed two regions of cell density: the outer region, being less dense, and the denser, inner region. This inner region is that which contains the portion of the foam that is re-entrant. It appeared that in some regions of the type HS 600 LDPE foam, having undergone the vacuum transformation, there were some slight regions of re-entrant structures, but for the most part, the foam seemed untransformed. Upon microscopic evaluation of the HS 900 foam, there was no buckling of the cell ribs.

As previously stated, the re-entrant structure appears to be found in the type HS 45 LDPE samples, and not in the types HS 600 and HS 900 LDPE samples. This is true for both methods of transformation.

Discussion

The transformation techniques employed on the PMI foams did not produce a re-entrant structure. SEM photographs revealed that after heat and compression were applied, the cell walls became thicker and some broke, instead of buckling inward. The uniform, orthogonally transformed PMI foams did exhibit an increase in both Young's modulus and shear modulus as the processing temperatures were increased. In comparing the transformed foam (PMI 51 WF) with its untransformed counterpart, their was a decrease in the calculated Poisson's ratio, from 0.39 to 0.33, yet this value was not the hoped-for negative value.

In the LDPE foam study, the least dense foam (HS 45), after appropriate processing, achieved a re-entrant structure, which in turn resulted in a negative Poisson's ratio. The re-entrant structure was obtained using both heat and hydrostatic pressure, as well as heat, vacuum pressure, followed by re-introduction of atmospheric pressure. The negative Poisson's ratio manifested itself anisotropically, only along one of the orthogonal directions, which may be attributed to the method of manufacturing the foam.

In order for one to observe the re-entrant structure, the outer layer of the foam sample had to be removed, or cored. Indeed, the core of the transformed sample had a higher volumetric compression factor than the outer region for both methods of transformation. The initial volumetric compression factors of this central region of the foams having undergone hydrostatic pressure and vacuum pressure treatments were, respectively, 2.41 and 2.73. These values are within the range of volumetric compression factors that Lakes(2) reported, 1.4 - 4.0. The other LDPE foam samples, HS 600 and HS 900, did not transform into a re-entrant structure. A possible explanation for this may be that since these materials were much stiffer than the HS 45, their cell ribs might have been able to rebound after heat and pressure were removed.

The successful transformation of the least dense LDPE foam samples brings to mind a possible application for this material, use in an artificial intervertebral disc. One could use this closed cell, re-entrant foam as a supplement to an artificial disc that would in essence be two plates, with a ball and socket joint between them. This foam could be used in a donut shape, to surround the ball and socket joint. This would serve several functions, tissue ingrowth into the joint would not occur, and wear debris from the joint would not escape into the rest of the body, both features attributable to the closed cell nature of the foam. Upon flexion of such an implant, due to the negative Poisson's ratio, there would be no outward bulging of the disc. Additionally, the foam can act as a means to resist flexion and rotation when attached to the superior and inferior endplates of the implant.

Conclusions

The combination of heat plus hydrostatic pressure did not result in the production of a re-entrant structure in the polymethacrylimide foams. However, this type of combination, as well as the combination of heat, vacuum pressure, followed by the re-introduction of atmospheric pressure, did yield a re-entrant structure in the HS 45 low density polyethylene samples.

References

1. Fung Y. C., Foundations of Solid Mechanics, Prentice-Hall, 1968

2. Lakes R. S., "Foam structures with a negative Poisson's ratio", Science, 235, 1987, 1038-1040

3. Friis E. A., Lakes R. S. and Park J. B., "Negative Poisson's ratio polymeric and metallic foams", J. Materials Science, 23, 1988, 4406-4414

4. Choi J. B. and Lakes R. S., "Non-linear properties of polymer cellular materials with a negative Poisson's ratio", J. Materials Science, 27, 1992, 4678-4684

5. Gere J. M. and Timoshenko S. P., Mechanics of Materials, Chapman & Hall, 1991

6. Lakes R. S., "Experimental microelasticity of two porous solids", Int. J. Solids, Structures, 22, 1986, 55-63

7. Chen C. P. and Lakes R. S., "Apparatus for determining the properties of materials over ten decades of frequency and time", J. Rheology, 33, 1989, 1231-1249

8. Brodt M., Cook L. S. and Lakes R. S., "Apparatus for measuring viscoelastic properties over ten decades: refinements", Rev. Sci. Instrum., 66, 1995, 5292-5297

9. Yasuda H. and Stannett V., Permeability coefficients. In Polymer Handbook, III-234 (edited by Brandrup J. and Immergut E. H.), John Wiley & Sons, New York, 1975

LIST OF FIGURES

Figure 1. Untransformed and re-entrant idealized foam cell structure modified from Choi and Lakes.(4) The term given for the geometry on the left is tetrakaidecahedron (14-sided polyhedron).

Figure 2. Micromechanics Apparatus in setup for testing Young's modulus and shear modulus: reprinted from Brodt et al.(8)

Figure 3. Material properties versus processing temperature of the compressed PMI 51 WF foam. All processing was performed at 552 kPa. Poisson's ratio was derived from E and G, based on equation (2).

Figure 4. The variation of the Poisson's ratio as a function of axial strain is shown here for the control sample of LDPE HS 45 foam.

Figure 5. Variation of Poisson's ratio as a function of axial strain is shown for a sample of LDPE HS 45 foam. This sample was transformed under 662 kPa and 110˚C for 10 hours, followed by 6 hours of 662 kPa pressure alone.

Figure 6. Variation of Poisson's ratio as a function of axial strain is shown for a sample of LDPE HS 45 foam. This sample was heated at 86˚C for one hour, then subjected to -82 kPa of pressure, and after 5 minutes, atmospheric pressure was suddenly restored.

Figure 7. Scanning electron micrograph of original PMI 51 WF foam (Magnification 128X). Length of scale mark is 3mm.

Figure 8. Scanning electron micrograph of transformed PMI 51 WF foam, processed at 170°C and 552 kPa for 8 hours (Magnification 128X). Length of scale mark is 3mm.

Figure 9. Scanning electron micrograph of transformed PMI 51 WF foam, processed at 220°C and 552 kPa for 8 hours (Magnification 128X). Length of scale mark is 3mm.

Figure 10. Scanning electron micrograph of original PMI 300 WF foam (Magnification 128X). Length of scale mark is 3mm.

Figure 11. A low magnification photograph of the cell structure of an untransformed LDPE HS 45 sample is shown; a scale is provided on the photograph.

Figure 12. A low magnification photograph of the cell structure of a transformed LDPE HS 45 (vacuum pressure) sample is shown; a scale is provided on the photograph.

Figure 13. A low magnification photograph of the cell structure of a transformed LDPE HS 45 (hydrostatic compressive pressure) sample is shown; a scale is provided on the photograph.

LIST OF TABLES

Table 1. Densities of various foams

Table 2. Various processing sequences and their respective volumetric compression factors for the LDPE and PMI foams

Table 3. Volumetric compression factors as a result of processing

Table 4. Material properties of two control (as claimed by the manufacturer) & two processed PMI foam samples

Figures

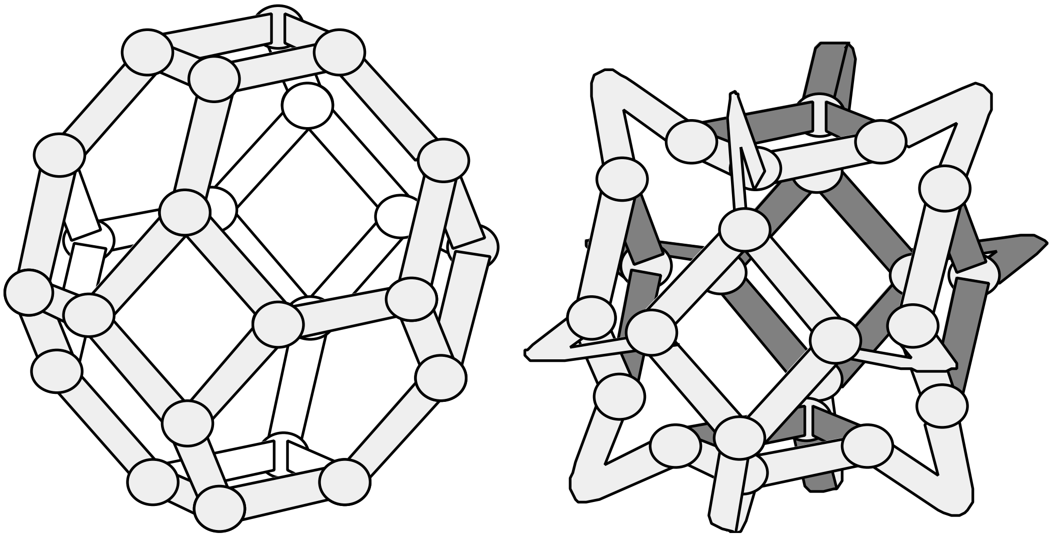

Figure 1. Untransformed (conventional, left) and re-entrant (right) idealized foam cell structure modified from Choi and Lakes.(4) The term given for the geometry on the left is tetrakaidecahedron (14-sided polyhedron).

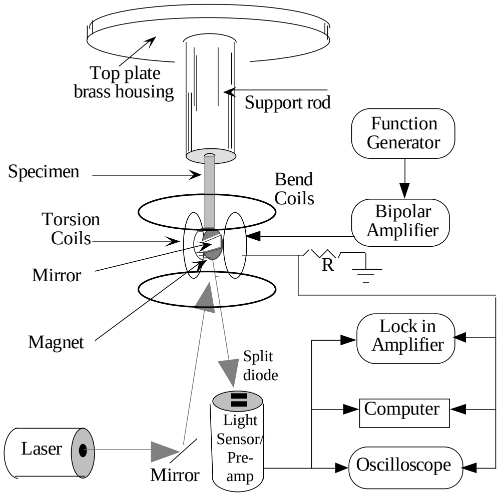

Figure 2. Micromechanics Apparatus in setup for testing Young's modulus and shear modulus: adapted from Brodt et al.(8)

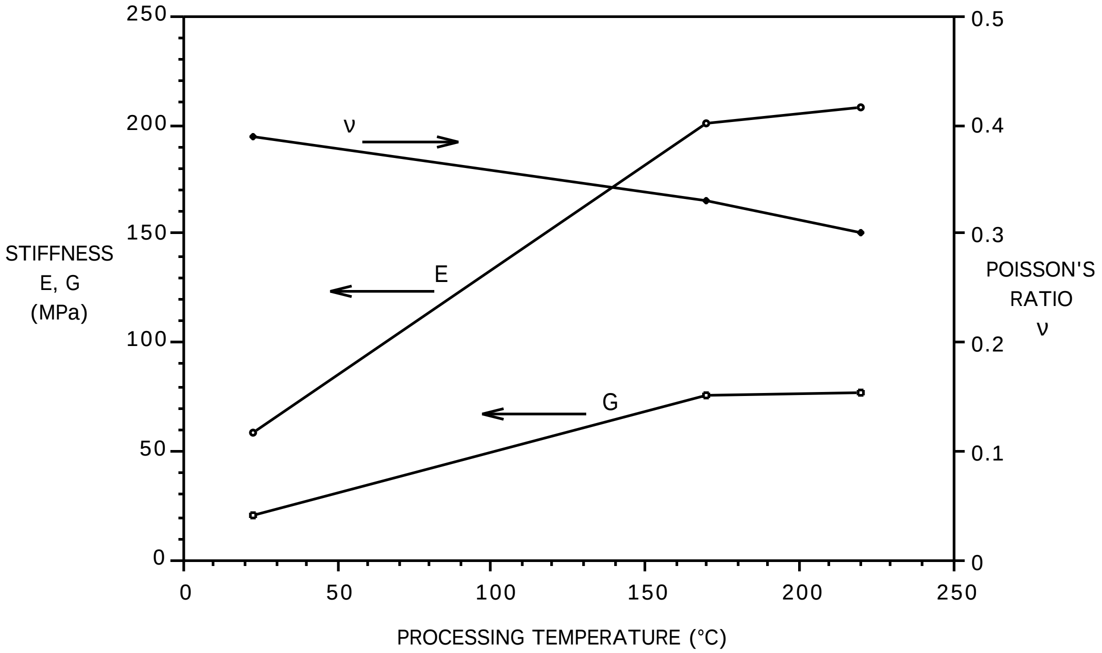

Figure 3. Material properties versus processing temperature of the compressed PMI 51 WF foam. All processing was performed at 552 kPa. Poisson's ratio was derived from E and G, based on equation (2).

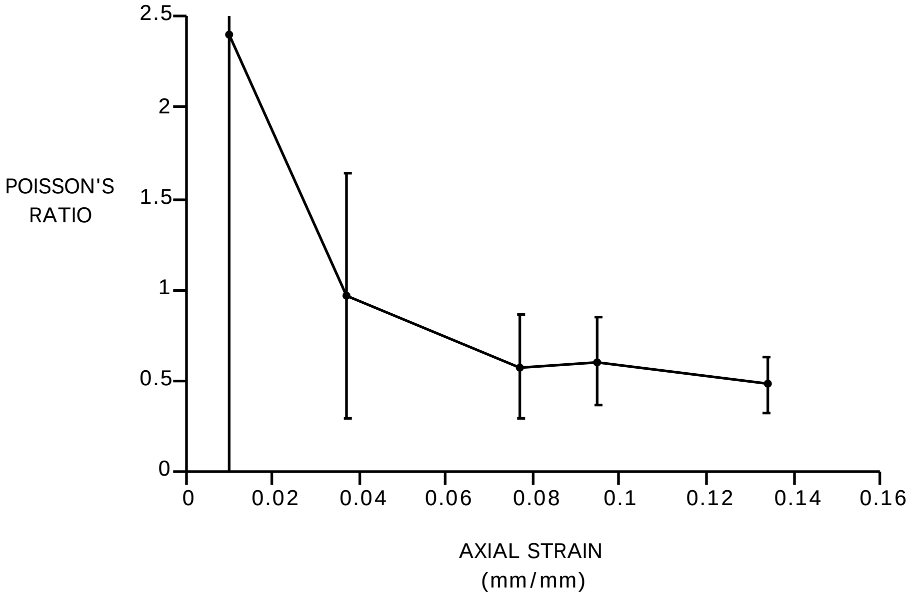

Figure 4. The variation of the Poisson's ratio as a function of axial strain is shown here for the control sample of LDPE HS 45 foam.

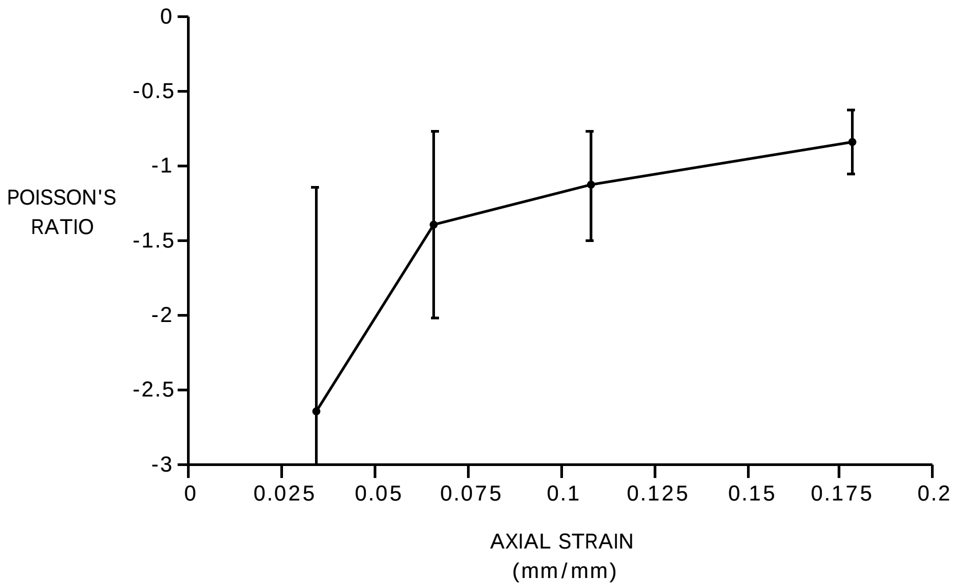

Figure 5. Variation of Poisson's ratio as a function of axial strain is shown for a sample of LDPE HS 45 foam. This sample was transformed under 662 kPa and 110˚C for 10 hours, followed by 6 hours of 662 kPa pressure alone.

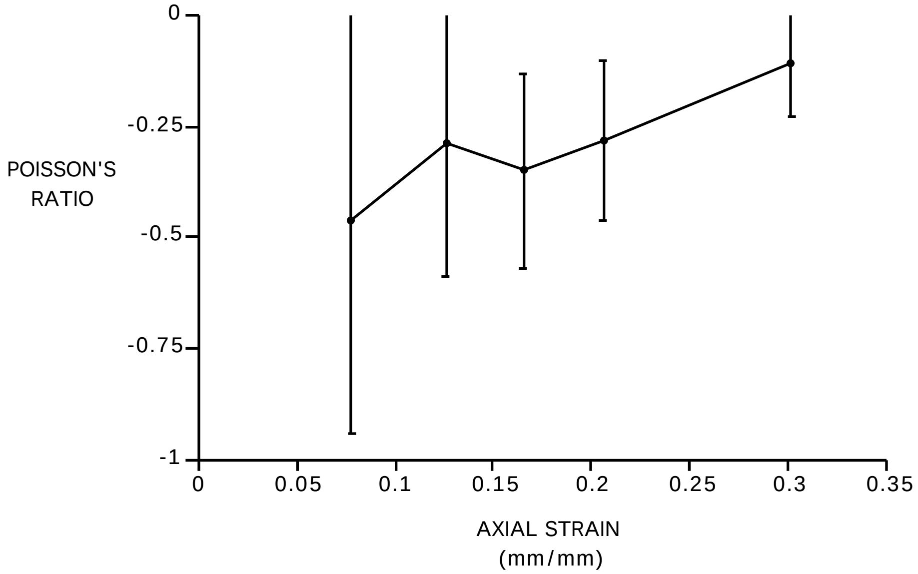

Figure 6. Variation of Poisson's ratio as a function of axial strain is shown for a sample of LDPE HS 45 foam. This sample was heated at 86˚C for one hour, then subjected to -82 kPa of pressure, and after 5 minutes, atmospheric pressure was suddenly restored.

see original article

Figure 7. Scanning electron micrograph of original PMI 51 WF foam (Magnification 128X). Length of scale mark is 3mm.

see original article

Figure 8. Scanning electron micrograph of transformed PMI 51 WF foam, processed at 170°C and 552 kPa for 8 hours (Magnification 128X). Length of scale mark is 3mm.

see original article

Figure 9. Scanning electron micrograph of transformed PMI 51 WF foam, processed at 220°C and 552 kPa for 8 hours (Magnification 128X). Length of scale mark is 3mm.

see original article

Figure 10. Scanning electron micrograph of original PMI 300 WF foam (Magnification 128X). Length of scale mark is 3mm.

see original article

Figure 11. A low magnification photograph of the cell structure of an untransformed LDPE HS 45 sample is shown; a scale is provided on the photograph.

see original article

Figure 12. A low magnification photograph of the cell structure of a transformed LDPE HS 45 (vacuum pressure) sample is shown; a scale is provided on the photograph.

see original article

Figure 13. A low magnification photograph of the cell structure of a transformed LDPE HS 45 (hydrostatic compressive pressure) sample is shown; a scale is provided on the photograph.

Table 1. Densities of various foams

Foam Type	Designation	Density (g/cm^3)
PMI Rohacell®	51 WF	0.052
	200 WF	0.205
	300 WF	0.301
LDPE Ethafoam®	HS 45	0.059
	HS 600	0.109
	HS 900	0.158

Table 2. Various processing sequences and their respective volumetric compression factors for the LDPE and PMI foams

Processing Condition	Foams			
	PMI 51 WF	PMI 51 WF	LDPE HS 45	LDPE HS 45
Temperature	170˚C	220˚C	110˚C	86˚C
Pressure	552 kPa	552 kPa	621 kPa	-86kPa
Time for Initial Heating	na	na	na	1 hour
Time for Heating Plus Pressure	8 hours	12 hours	10 hours	5 minutes
Time for Pressure Alone			6 hours	na

na: not applicable. This item was not used in, or measured after, the processing sequence for the foam sample in question.

Table 3. Volumetric compression factors as a result of processing

Volumetric Compression Factor	Foams			
	PMI 51 WF	PMI 51 WF	LDPE HS 45	LDPE HS 45
Overall	2.0[a]	8.0[b]	1.44[c]	2.21[e]
Inner Region of Foam	na	na	2.41[c] 3.38[d]	2.73[e] same[e]
Outer Region of Foam	na	na	1.36[c] 1.89[d]	1.73[e] same[e]

na: not applicable. This item was not used in, or measured after, the processing sequence for the foam sample in question.

a: Immediately after processing at 170˚C and 552 kPa for 8 hours

b: Immediately after processing at 220˚C and 552 kPa for 12 hours

c: Immediately after processing at 110˚C and 621 kPa for 10 hours

d: Three weeks after processing at c

e: Immediately, as well as three weeks after, processing at 86˚C and -86 kPa

Table 4. Material properties of two control (as claimed by the manufacturer) & two processed PMI foam samples

Samples	Young's Modulus (MPa)	Shear Modulus (MPa)	Calculated Poissons Ratio	Density (g/cm^3)
51 WF Control (200WF)	58.76 ± 3.78	21.07 ± 0.93	0.39 ± 0.04	0.061 ± 0.006
51 WF Compressed (170°C)	200.34 ± 22.47	75.71 ± 10.60	0.33 ± 0.09	0.168 ± 0.004
51 WF Compressed (220°C)	207.55 ± 15.07	77.54 ± 8.77	0.30 ± 0.13	0.195 ± 0.004
200 WF Control	259.93 ± 8.92	149.96 ± 2.52	-0.12 ± 0.03	0.205 ± 0.008

Note: Tests were conducted at room temperature. Standard deviations for each value are reported as well.